Article **Journal of Innovative Engineering**
December 2022, Vol.6 No.19 13-25

Modeling of a control system for the boost-boost converter in photovoltaic applications

Modelado de un sistema de Control para el convertidor elevador-boost en aplicaciones fotovoltaicas

MÉNDEZ-DÍAZ, Juan Francisco†, SÁNCHEZ-RUIZ, Francisco Javier, MUÑOZ-JARILLO, Carlos Rene and ROSANO-ORTEGA, Genoveva

Universidad Poular Autónoma del Estado de Puebla, Mexico.

ID 1st Author: *Juan Francisco, Méndez-Diaz* / **CVU CONACYT**: 292499

ID 1st Co-author: *Francisco Javier, Sánchez-Ruiz* / **CVU CONACYT**: 169828

ID 2nd Co-author: *Carlos Rene, Muñoz-Jarillo* / **CVU CONACYT**: 976861

ID 3rd Co-author: *Genoveva, Rosano-Ortega* / **CVU CONACYT**: 100557

DOI: 10.35429/JOIE.2022.18.6.13.25 Received March 13, 2022; Accepted June 30, 2022

Abstract

The boost-boost converter presents interesting characteristics for photovoltaic applications, due to the nature of the system where we can increase the voltage in an adequate and controlled way according to the load, in combination with an optimal control system we can obtain a better efficiency of a autonomous photovoltaic system, according to the above, this article deals with the low voltage photovoltaic application of an isolated system, using a boost-boost converter and a PI control system using two different solar panels, with the aim of showing that with a PI control we can obtain good efficiency of the two systems even with the presentation of disturbances as well as if a more robust control is implemented in photovoltaic applications, saving both operating cost and implementation time. The I-V characteristics similar to a non-linear source of the photovoltaic module, require the inclusion of linearization of the photovoltaic module and with this to be able to design the control of the system, the proper functioning of the designed control has been tested through mathematical modeling and simulation.

Autonomous, application, modeling

Resumen

El convertidor elevador-boost presenta características interesantes para aplicaciones fotovoltaicas, debido a la naturaleza del sistema donde podemos aumentar el voltaje de una manera adecuada y controlada de acuerdo a la carga, en combinación con un sistema de control optimo podemos obtener una mejor eficiencia de un sistema fotovoltaico autónomo, de acuerdo a lo anterior en este artículo se aborda la aplicación fotovoltaica en bajo voltaje de un sistema aislado, utilizando un convertidor elevador-boost y un sistema de control PI usando dos sistemas fotovoltaicos diferentes, con el objetivo de mostrar que con un control PI esencial podemos obtener buena eficiencia de los dos sistemas aun con presentación de perturbaciones al igual que si se implementara un control más robusto en aplicaciones fotovoltaicas ahorrando tanto costo de operación como tiempo en la implementación. Las características I-V similar a una fuente no lineal del módulo fotovoltaico, requieren la inclusión de linealización del módulo fotovoltaico y con esto poder diseñar el control del sistema, el buen funcionamiento del control diseñado ha sido probado mediante el modelado matemático y por simulación.

Autónomo, Aplicación, Modelado

Citation: MÉNDEZ-DÍAZ, Juan Francisco, SÁNCHEZ-RUIZ, Francisco Javier, MUÑOZ-JARILLO, Carlos Rene and ROSANO-ORTEGA, Genoveva. Modeling of a control system for the boost-boost converter in photovoltaic applications. Journal of Innovative Engineering. 2022. 6-19:13-25.

*Correspondence to Author (E-mail: juanfrancisco.mendez@upaep.mx)
† Researcher contributing as first Author.

© ECORFAN- Republic of Perú

Introduction

In recent years, the demand for energy has increased continuously, with the main source being the indiscriminate use of fossil fuels. This constantly growing energy demand has generated an increase in greenhouse gases, causing severe damage to the environment, such as global warming and the worldwide problem of climate change. Thus, in the global energy context, renewable energies have emerged as a response to the social demand to reduce CO_2 emissions and other pollutants of direct action.

Photovoltaic systems are one of the most studied models for obtaining electricity from renewable sources. According to (Ram, et al., 2017), when using photovoltaic systems for energy production, one of their particularities is the fact that the electrical voltage generated by the photovoltaic panels has a non-linear relationship with irradiation in such a way that the maximum voltage generated does not represent the maximum power that the panel can deliver to an electrical load. Given this non-linearity, the maximum power that the PV panel can deliver is a function of the combination of voltage and current in the electrical load.

This non-linearity presented by the solar panels tries to be solved by determining an operating point or maximum power point (MPP) as long as it is under standard measurement conditions (STC), the STC according to the literature the solar panel must have a temperature of 25°C and an irradiation of 1000 W/m2 on the surface of the panel. The performance of the most promising PV technology should be regulated according to the MPP. The output of the PV system is affected by temperature, irradiation and partial shading conditions, these changes in environmental conditions limit the efficiency and power output of the panel and the measured output of the panel deviates from the desired set point. To improve the MPP there is the maximum power point tracker (MPPT) as it estimates and controls the MPP, the design of the MPPT system to achieve a regulated output is done by voltage converters and controllers to converge the MPP even under distribution conditions. There are different types of converters and controllers to optimise the efficiency of the PV panel using MPPT (Sharma & Jain, 2015).

According to Ebrahimi & Viki, (2015) DC-DC converters are widely used in renewable energy generation systems such as solar PV systems, wind systems and fuel cells in order to obtain correct power conversion as shown in figure (1).

Solar photovoltaic (PV) power generation system is used in grid-connected applications and stand-alone or islanded system (Saravanan & Ramesh Babu, (2017). In Alam & Hoque (2019) it is proposed that the most suitable power converter to solve the problem of low voltage levels obtained from PV panels, is the boost-boost converter; which raises and regulates the output voltage. The input of the boost converter acts as a current source due to the input inductor, which means that it has almost constant input current, which is favourable in PV systems. By interleaving boost converters, low ripple current is achieved in the input current, output voltage and high power conversion. This topology can be used for the interface connection between the low voltage of the PV array and a high input voltage of the battery bank or any DC load (Taghvaee, et al., 2013).

The boost-boost converter helps to increase the voltage level, improve stability and power factor. In some cases, the converter can also be used as a pre-regulator. It is clear that the DC-DC converters require an acceptable and efficient operation for the PV system to be effective and have the least possible energy losses, this also depends directly on the control used in the system and ensure the smooth operation of the system even with the presentation of disturbances.

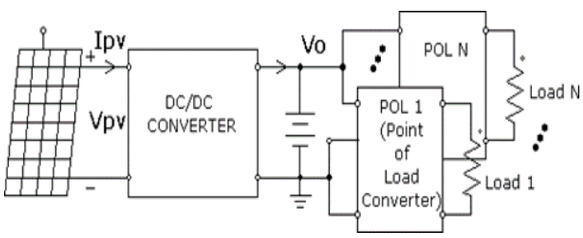

Figure 1 Photovoltaic system architecture with serial DC bus
Source: Méndez et al., 2014

ISSN 2523-6873
ECORFAN® All rights reserved.

Another application of boost-boost converter is proposed in Dhople et al., 2009, where three boost converters are interleaved where superior current characteristics were found compared to the coupled converters. In Tian et al., 2016, they use an improved interleaved boost-boost circuit, concluding that this is the most suitable for PV using an MPPT algorithm, as it has greater advantages than the traditional interleaved boost converter (TIBC) and single boost converter (SBC) such as:

- Higher set-up ratio.
- More stable, accurate output voltage with less ripple.
- Lower switch voltages.
- It is useful to increase system efficiency and reduce energy losses.

But for the operating system to work properly, a control model needs to be developed to allow the system to operate properly. Among the control systems for photovoltaic applications with switched DC/DC converters are Proportional Integral Derivative (PID) and Proportional Integral (PI). According to Dwivedi & Saket (2017), in PV system the value of maximum power, current and peak voltage are increased by controlling the gain of the PID controller. In Rabiaa et al., (2019) a cascaded closed loop control using PI controller is proposed for DC-DC boost converter showing good performance in terms of rise time, disturbance rejection and steady state error. Furthermore, it is shown that the DC-DC boost converter has a strongly non-linear dynamic behaviour, so that the performance of any linear controller such as the PI controller can only be optimal as long as the system remains around a certain operating point, i.e. for photovoltaic applications, where solar panels are characterised by their non-linear structure, and if a PI or PID control is to be applied, which are controls characterised by using linearised models around an equilibrium point, the behaviour of the solar panels must be linearised by means of their basic equation. If this were not the case and it were desired to work with the non-linear structure, other control modes would have to be used, such as the sliding mode control used (Méndez, et al., 2014; Méndez, et al., 2015; Méndez, 2018 and Méndez, et al., 2019).

Therefore, this article presents the analysis of the boost-boost converter used in two photovoltaic systems, implementing a PI control system, with the aim of showing that with an essential control like this, widely used in various systems, we can obtain optimal control performance in the event that disturbances occur, as well as if a more robust control is implemented, reducing costs and operating times. In our application we can obtain the control of the input voltage V_PV of two different photovoltaic panels, taking into account the parasitic losses that occur in a real system, together with the non-linearity representative of the photovoltaic panels, and taking into consideration the linearisation of the models of both panels and working them around an equilibrium point, thus obtaining the maximum of their power even with perturbation, we obtain an optimal response of both systems. The analysis is performed with two different panels with powers of 85W and 100W, for the 85W panel was taken as a reference from the article Méndez et al., (2015), where they use the same panel.

The objective of this work can be listed as follows:

To present a general approach to derive in the transfer function of the boost-boost DC-DC converter and achieve system control in both solar panels.

Present a PI controller design approach for the input voltage of the PV panels to achieve a constant output voltage independent of the load variation.

Present the controller implementation using mathematical modelling and the control system to verify the results of each design.

To demonstrate that with a control system such as the PI it is possible to obtain satisfactory results in two types of solar panels with different powers, and that these respond appropriately in the event of disturbances in the system.

ISSN 2523-6873
ECORFAN® All rights reserved.

Theoretical analysis

Boost converter

The circuit diagram of the boost converter, as shown in figure (2), consists of an electronic switch that is controlled by a PWM signal. The inductor stores the energy coming from the source until the Ton period when the electronic switch is turned on. Meanwhile, when the diode is reverse biased it isolates the output of the circuit and the load current is supplied from the capacitor (Méndez, et al., 2014). When the electronic switch is off, the inductor is discharged and current flows through the diode. The output voltage is composed of the discharged voltage and the instantaneous panel voltage, so it is always higher than the input voltage. The switching on and off of the switch is controlled by the PWM signal (Bouchakour et al., 2015).

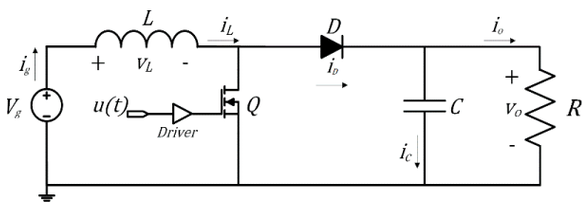

Figure 2 Boost converter schematic
Source: Mendez, 2018.

According to the above, for the research presented in this article, one of the elementary converters will be used, the boost converter, in combination with the solar panel and a battery which will have a linear behavior as shown in figure (3), applying a PI type control.

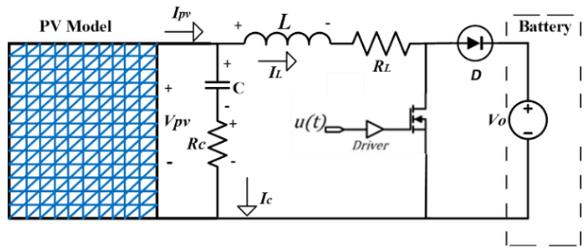

Figure 3 Behavior of a solar panel and its battery with a boost converter
Own source.

Photovoltaic panel analysis

Photovoltaic panels are non-linear systems, since as expressed in Leuchter, et al, (2012) there is a performance loss that is distributed non-linearly and parametrically (with solar irradiance and temperature) along the voltage axis of the panel, i.e. the direct application of the Shockley equation, I=Io*[e^((v/(n*Vt)))-1] in every panel does not give good modelling results, and the main reason is the existence of power losses that are spread along the voltage axis in a non-linear way.

In addition to these facts, the quality of the semiconductor material n is also variable and depending on the manufacturing process, the semiconductor material, the solar radiation and the temperature, the efficiency of the system depends a lot, so when you want to connect it with a DC/DC converter it is necessary first to linearise the photovoltaic panel and then linearise the converter, the technique to linearise the converter will be by means of state space analysis. For the analysis of the PV systems we use the parameters of the specification sheets of each of them, and the classical simplified model of the i-v relationship of the PV module (Méndez, et al., 2015).

$$i\_pv=i\_sc-I\_R*e^{(a*v\_pv)} \quad (1)$$

The classical solar panel equation as shown in equation 1 is interpreted as follows: i_pves is the current supplied by the PV module, i_s is the short circuit current which depends on the irradiance, v_pv is the operating voltage of the module, I_R*e^a are parameters of the PV module which depend on multiple technological factors and temperature, as shown in figure (4a).

To linearise the system we represent it as shown in figure (4b), where the resistor will have the same current and voltage as the classical PV model as found in equation 2, always working at the maximum **power point of the MPPT panels.**

$$Rpv = \frac{Vmpp}{Ipv - Impp} \quad (2)$$

ISSN 2523-6873
ECORFAN® All rights reserved.

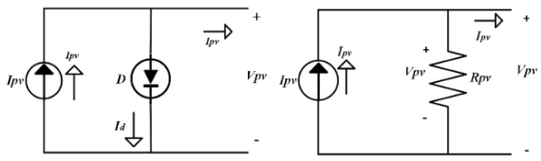

Figura 4a. **Figura 4b.**

Figure 4 Sample of a photovoltaic module with current and voltage variation
Source: Own elaboration

Based on the above, the linearised Norton model is used for the system analysis together with the boost converter as shown in figure (5), in order to perform the mathematical modelling, around the MPPT maximum power point as proposed by Hogan (2014). Circuits comprising arbitrarily complicated sets of voltage sources, current sources, resistors, capacitances and inductances can be represented by Norton equivalent circuits.

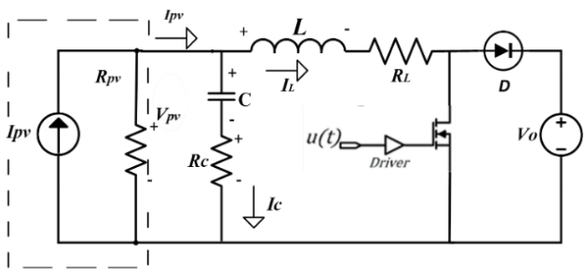

Figure 5 Norton model in a boost converter
Source: Own elaboration

A. Mathematical analysis

For the mathematical analysis of the system, the objective is to control the input voltage of the photovoltaic panel and produce the maximum power, based on the boost converter considering the losses in both the inductor and the capacitor by adding the series resistors in each of the devices.

For the analysis of the system we will perform it in its two operating points according to the boost converter as shown in figure (5).

To obtain the averaged system we analyse the boost-boost converter first in switched mode in its two operations obtaining the following equations:

$$\begin{cases} u = 1 \; en \; state \; on \\ u = 0 \; in \; state \; off \end{cases}$$

"$\boldsymbol{u = 1}$" Iinterval 1 (switch closed ON)

$$L\frac{dI_L}{dt} = V_C + I_C \; x \; R_C - I_L \; x \; R_L \qquad (3)$$

$$C\frac{dV_C}{dt} = I_C = \; I_{PV} - I_L \qquad (4)$$

"$\boldsymbol{u = 0}$" interval 2 (switch opened OFF)

$$L\frac{dI_L}{dt} = V_C + I_C \; x \; R_C - V_O - I_L \; x \; R_L \qquad (5)$$

$$C\frac{dV_C}{dt} = I_C = \; I_{PV} - I_L \qquad (6)$$

Taking into consideration that the current generated by the Norton model in figure (5) I_PV for the solar panel and the voltage of the same model V_PV are not equations of state as shown in equations (4) and (6) in the analysis of the interval when u=1 and u=0, these will have to be equated so that the current and voltage of the model are an equation of state, by equating these two variables with respect to the Norton model in figure (5) we are left with the following equations:

$$I_{PV} = \; I_{SC} - \frac{V_{PV}}{R_{PV}} \qquad (7)$$

$$V_{PV} = \; V_C + I_C \; x \; R_C \qquad (8)$$

Substituting equation (7) and (8) into (4) we obtain the following equation which is the same for both system states

$$C\frac{dV_C}{dt} = \frac{1}{R_{PV} + R_C}(I_{sc} \; x \; R_{PV} - I_L \; x \; R_{PV} - V_C) \qquad (9)$$

By performing the relevant operations on equations (3) and (5) for the inductor and (9) for the capacitor in the boost converter, the averaged model looks as follows, where the equations are already a function of the system inputs:

$$L\frac{dI_L}{dt} = \; V_C + I_C \; x \; R_C - I_L \; x \; R_L - V_O \; x \; (1 - d) \qquad (10)$$

$$C\frac{dVc}{dt} = \frac{1}{R_{PV} + R_C}(I_{sc} \; x \; R_{PV} - I_L \; x \; R_{PV} - V_C) \qquad (11)$$

For the steady state analysis, we again consider the Norton model of figure (5) where we analyse the following points according to the electrical structure of the PV system: taking into account that the average capacitor current is zero, we obtain that the inductor current will be equal to the PV panel current and the maximum power current, the same would be for the panel voltage which will be equal to the capacitor voltage and the maximum power voltage, thus obtaining the following equations (12 and 13).

ISSN 2523-6873
ECORFAN® All rights reserved.

$$I_L = I_{PV} = I_{MPP} \quad (12)$$

$$V_C = V_{PV} = V_{MPP} \quad (13)$$

From the above we can also derive the duty cycle by equating equation (10) to zero and obtain the following equation (14).

$$D = 1 - \frac{V_{MPP} - I_{MPP} * R_L}{Vo} \quad (14)$$

Based on the averaged model, the equations of state and the steady state analysis, we can perform the mathematical modelling using state space analysis, this analysis is performed for both solar panels, where we define the state vectors x which are the inductor current I_L and the capacitor voltage V_C , the input vectors u, which are the duty cycle d the output voltage V_O together with the panel current I_PV and the control variable y which is the PV panel voltage V_PV as shown in the following equation.

$$x = \begin{bmatrix} I_L \\ V_C \end{bmatrix} \qquad u = \begin{bmatrix} d \\ V_O \\ I_{PV} \end{bmatrix} \qquad y = [V_{PV}] \quad (15)$$

According to equations (10) and (11) to the vectors presented in (15), the matrix δ will give us the relationship that exists between the functions and the states, as follows:

$$\delta = \begin{bmatrix} \left(\frac{1}{L}\right) * \left(\frac{-R_{PV} * R_C}{R_{PV} + R_C}\right) - R_L & \left(\frac{1}{L}\right) * \left(1 - \frac{R_C}{R_{PV} + R_C}\right) \\ \left(\frac{1}{C}\right) * \left(\frac{-R_{PV}}{R_{PV} + R_C}\right) & \left(\frac{1}{C}\right) * \left(\frac{-1}{R_{PV} + R_C}\right) \end{bmatrix}$$

Taking equations (10) and (11) with respect to the input vectors $u = \begin{bmatrix} d \\ V_O \\ I_{PV} \end{bmatrix}$ For the matrix β which gives us the relationship between the function and the inputs we get:

$$\beta = \begin{bmatrix} \left(\frac{1}{L}\right) * V_O & \left(\frac{1}{L}\right) * (-1 - d) & \left(\frac{1}{L}\right) * R_C \left(\frac{R_{PV}}{R_{PV} + R_C}\right) \\ 0 & 0 & \left(\frac{1}{C}\right) * \left(\frac{R_{PV}}{R_{PV} + R_C}\right) \end{bmatrix}$$

For the matrix γ, having the variable to be controlled y=[V_PV] as a function of the states x=["(I_L@V_C)] we obtain :

$$\gamma = \begin{bmatrix} R_C \left(\frac{-R_{PV}}{R_{PV} + R_C}\right) & 1 - \frac{R_C}{R_{PV} + R_C} \end{bmatrix}$$

For matrix D having the variable to be controlled and = $[V_{PV}]$ en function of the inputs $u = \begin{bmatrix} d \\ V_O \\ I_{PV} \end{bmatrix}$ we obtain:

$$\varepsilon = \begin{bmatrix} 0 & 0 & R_C \left(\frac{R_{PV}}{R_{PV} + R_C}\right) \end{bmatrix}$$

As we can see the state space analysis shows us the complete behaviour of the system obtaining the transfer functions for both photovoltaic panels, these will be explained in the following section.

Comparison between Proportional, Proportional Integral and Proportional Integral Derivative Controls

As we know, in order to control a variable of a switched converter, it is necessary that the switched converters have a closed loop control system as shown in figure (6), where 4 components can be observed, 1) the main component which is the switched converter, 2) the block that calculates the error of the switching converter, 3) the block that calculates the error of the switching converter, 4) the block that calculates the error of the switching converter, and 5) the block that calculates the error of the switching converter, 2) the block that calculates the voltage error e(t) which is indispensable for the comparison of the system between those to be controlled, 3) the control component which mainly acts on the error by amplifying it and 4) the modulator which transforms the controller output into digital signals which are applied directly to the switches of the switched converter. Sometimes the modulator block is considered to be part of the controller block or the plant itself (Méndez, 2018).

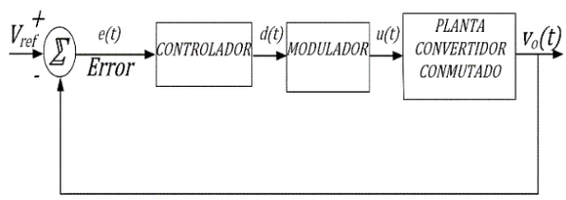

Figure 6 Control block diagram of a switched regulator.
Source: Méndez, 2018

ECORFAN® All rights reserved.

Based on the above for the control design and taking into consideration that we will have to control the input voltage of the solar panel according to the Norton model, we start with the comparison between the different control systems, explaining why the integral proportional control is the best suited to the needs of the photovoltaic system, for this according to the mathematical analysis previously explained in the previous section we first show the application of proportional control.

PROPORTIONAL CONTROL PANEL 85W.

Once the proportional control has been applied, we can see the following:

In figure (7) working in closed loop we can see that it is divided in three parts, the step response, the geometrical place of the roots and the Bode diagram: In the Bode diagram as can be seen when applying the proportional control the bandwidth never reaches the final value which is marked by the black line and is the value indicated by the control, in the geometric place of the roots we can observe according to the damping marked by the black lines that the closed loop poles also do not approach the damping indicated by the control system even changing the value of the proportional constant, and even though we see that the response over time reaches a certain stability, at start-up it tends to be oscillatory, so we conclude that proportional control is not a good option for implementation in our system.

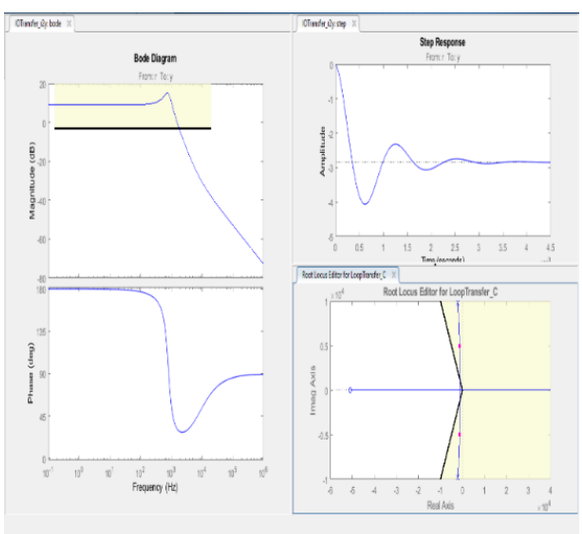

Figure 7 Application of Proportional Control.
Source: Own elaboration

Proportional integral derivative control panel 85w

When the proportional integral derivative control is applied, we can see the following: In the same way we analyse the system presented in figure (8), as we can appreciate in the Bode diagram the bandwidth does reach the value marked by the control line, but although it complies in this way graphically we can observe that the response is not optimal, in the geometric place of the roots we see that the closed loop poles are not close to the damping marked by the black lines, and the response in time as well as the proportional control finds certain stability but the response at the beginning of the system also presents certain oscillation.

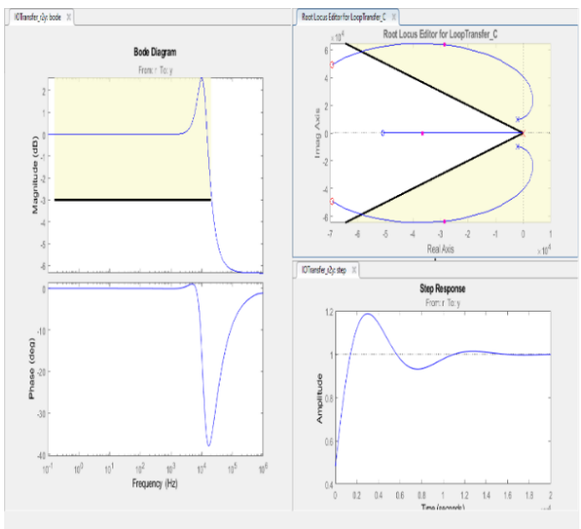

Figure 8 Application of Derivative Proportional Integral Control
Source: Own elaboration

Integral proportional control panel 85w

When the integral proportional control is applied, we can see the following: According to the figure (9) the same as the two previous controls it is shown in the Bode diagram the bandwidth where this if it arrives to the value marked by the control line, the same as the PID control but it can be observed that the response is optimal, in the geometric place of the roots we see that the poles of closed loop now if they are positioned directly in the lines of the damping marked by the control, and the response in time presents a stability and an optimal response for the control system, so we can conclude that the PI control compared to the other controls is the optimum in all operating conditions that marks the control system designed.

ISSN 2523-6873
ECORFAN® All rights reserved.

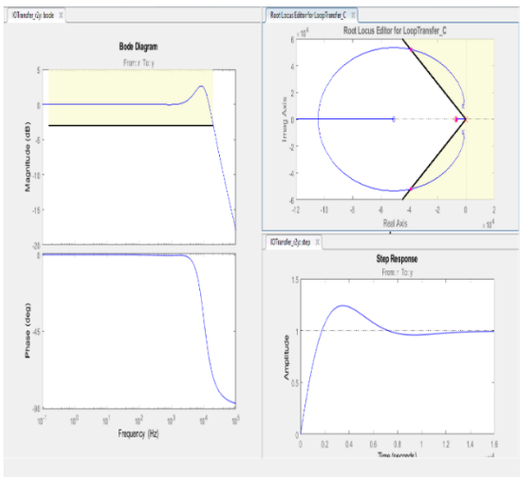

Figure 9 Application of Proportional Integral Control.
Source: Own elaboration

Proportional control panel 100

When proportional control is applied, the following can be seen:

In figure (10) the same as in the 85W panel working in closed loop: In the Bode diagram as it is observed when applying the proportional control the bandwidth never reaches the final value which is marked by the black line and is the value indicated by the control, in the geometric place of the roots we can observe according to the damping marked by the black lines that the closed loop poles also do not approach the damping indicated by the control system even changing the value of the proportional constant we do not have a significant approach, and even though we see that the response over time reaches a certain stability, at start-up it tends to be oscillatory, so we conclude that proportional control is not a good option for implementation in our system, very similar to the behaviour in the 85W panel.

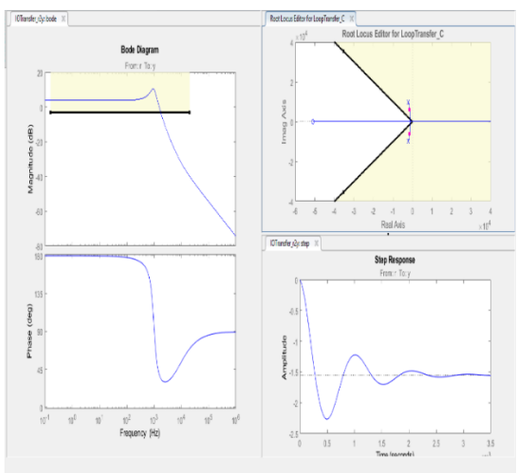

Figure 10 Application of Proportional Control 100W
Source: Own elaboration.

Proportional integral derivative control 100w panel

When the proportional integral derivative control is applied, we can see the following:

In the same way we analyse the system presented in figure (11), very similar to the behaviour of the 85W panel so we will summarise it a little, the Bode diagram the bandwidth does reach the value marked by the control line, but although it complies in this way graphically it can be seen that the response is not optimal, in the geometrical place of the roots, the closed loop poles are not close to the damping marked by the black lines, and the response in time as well as the proportional control finds some stability but the response at the beginning of the system also presents some oscillation.

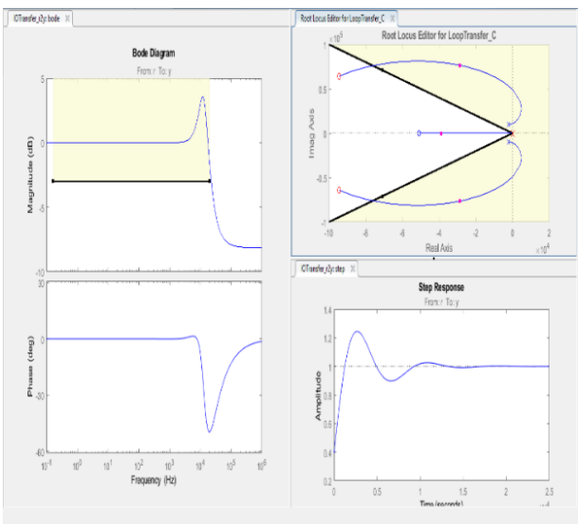

Figure 11 Application of Proportional Integral Derivative Proportional Control 100W
Source: Own elaboration.

Proportional integral control panel 100w

When the integral proportional control is applied, we can see the following:

ECORFAN® All rights reserved.

According to the figure (12) following the same thematic and observing that the control the behaviour of the control also is very similar to the panel of 85 W we can appreciate that in the diagram of Bode the bandwidth if it arrives to the value marked by the control line, the same as the PID control but it can be observed that the response is optimal, In the geometric location of the roots we can see that the closed-loop poles are now positioned directly on the damping lines marked by the control, and the response in time presents stability and an optimum response for the control system, so we can conclude that the proportional integral control is the most optimum for both panels as it meets the operating conditions required by the control system.

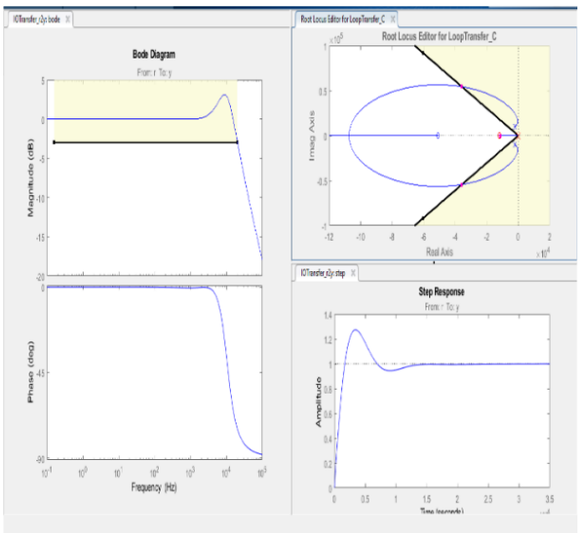

Figure 12 Application of Integral Proportional Control 100W
Source: Own elaboration

Application of the control systems

Based on Méndez, et al., (2015) for the analysis of the first panel we obtain the following technical characteristics; the photovoltaic panel is a module of 85 W, with nominal parameters at 25 ºC and 1 kW / m2 of: *I*SC = 5 A, *V*oc = 22.1 V, *I*MPP = 4.72 A, *V*MPP = 18 V. For the second panel which has the following technical characteristics; the 100 W photovoltaic panel has nominal parameters at 25 ºC and 1 kW / m2 of: *I*SC = 5.86 A, *V*OC = 22.3V, *I*MPP = 5.38 A, *V*MPP = 18.6 V. After the relevant analyses to obtain the boost converter parameters, the values for each of the components are as follows: L=75µH, RL=150mΩ, C=75µF, RC=196.3mΩ.

Obtaining the transfer functions by performing the previous analysis of the boost converter modelling and linearising around the operating point in both photovoltaic panels is as follows:

For the 85W panel

$$Gvd = \frac{-62641(s + 6.791 * 10^4)}{s^2 + 4817s + 1.776 * 10^8}$$

For 100W panel

$$Gvd = \frac{-62515(s + 6.791 * 10^4)}{s^2 + 4947s + 1.776 * 10^8}$$

As we can see both transfer functions are very similar, both show that the system is stable, but they present a negative gain, so the system could present some instability, because of this the control design becomes more complex, as it is left with a positive feedback. The control design now has to compensate or cancel the negative gain of the system, and thus have a stable system. By compensating the gain and as shown in the diagrams above from the comparison of the different controls we get the following transfer functions

For the 85w panel

$$Gcv = \frac{-1.6317s - 6773}{s}$$

Fort he 100w panel

$$Gcv = \frac{-1.7511s - 1.42 * 10^4}{s}$$

By obtaining the above transfer functions and with the control system applied, we observe that it is completely stable, which allows the objective of the control system to be achieved, which is to regulate the input voltage of the photovoltaic panel following a reference voltage, always looking for the point of maximum power. As shown in the following graphs, we start with the 85 W panel and then the 100 W panel.

ISSN 2523-6873
ECORFAN® All rights reserved.

As we can see in the figure (13) and (14) we can see that the panel operates in a suitable way, with which we verify that the linearization of the same one is the correct one since it is on the 18V that is the optimal voltage of operation of the panel according to its technical card in the same way that the current of the panel Ipv with a value of 4.72 A that is the optimal value of operation according to the technical card of the panel, and also we can observe that it is the equal to the current of the inductor, also fulfilling the analysis in stationary state IL.

For 85 W panel

Steady state analysis

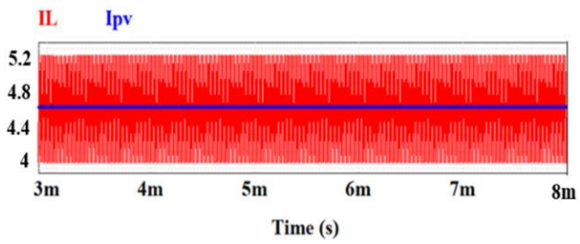

Figure 13 Steady state analysis
Source: Own elaboration

Implemented Control System

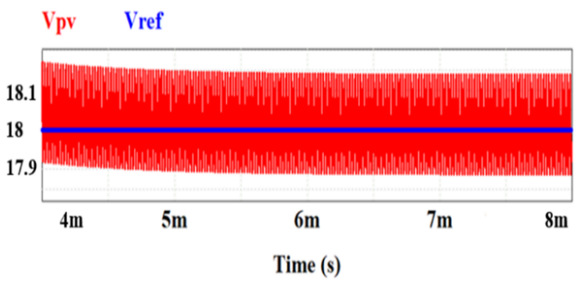

Figure 14 Panel voltage Vpv and reference voltage vref
Source: Own elaboration

In figure (14) we can see that the control operates properly since the panel voltage Vpv follows without problems the reference voltage Vref equal to 18V, always guaranteeing the maximum power point. Figure (15) shows a direct disturbance to the system simulating a partial shading in the solar panel of almost 70%, the control when presenting this disturbance, adapts almost immediately and responds again in an optimal way, where it is seen that the voltage Vpv of the solar panel after the disturbance follows without problems to the reference voltage Vref always over 18 V, taking into account that this is a fairly high disturbance the control continues to respond adequately.

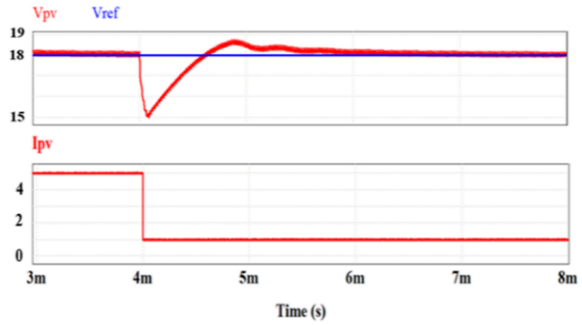

Figure 15 Disturbance present simulating partial shading
Source: Own elaboration

Figure 16 shows another disturbance which shows an increase in the battery voltage due to the load coming from the photovoltaic panel and as can be seen there is an increase in the output voltage Vo from 24V to 27V and again the solar panel voltage Vpv follows without any complication the reference voltage Vref always over 18V adapting quickly after the disturbance.

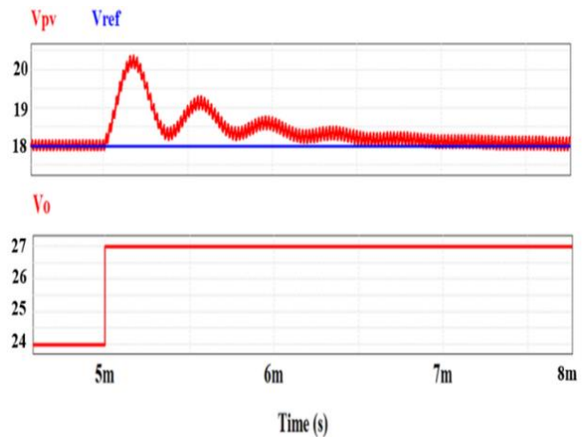

Figure 16 Second disturbance present in the battery.
Source: Own elaboration

In the same way that in the 85W solar panel we can see in the figure (17) and (18) now with the 100W solar panel, we can see that the panel operates in an adequate way, with which we also verify that the linearisation of the same is correct since it is over 18.6 V and the panel current Ipv is equal to the inductor current IL, also verifying the optimum analysis in steady state.

ISSN 2523-6873
ECORFAN® All rights reserved.

100W panel

Steady state analysis

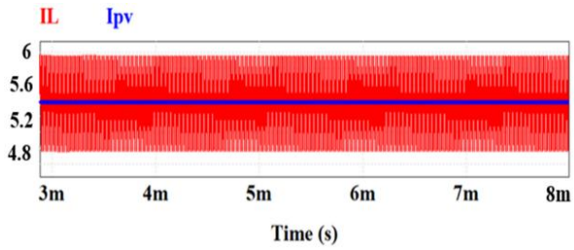

Figure 17. Steady state analysis
Source: Own elaboration

Implemented Control System

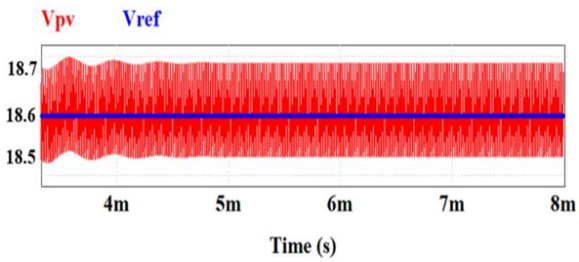

Figura 18 Panel Voltage Vpv and Reference Voltage Vref.
Source: Own elaboration

In the same way as in the previous panel in figure (18) we can see that the control operates properly as the panel voltage Vpv follows smoothly the reference voltage Vref now at 18.6V, always guaranteeing the maximum power point, and the stability of the system.

In figure (19) we repeat the same disturbance of the 85W panel causing a partial shading of the same magnitude now in the 100W panel, as we can observe the current Ipv drops its amperage suddenly and considerably, and the control continues to operate correctly, showing the good performance also for this panel.

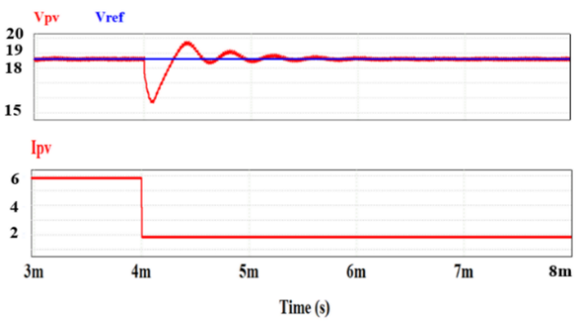

Figure 19 Disturbance present simulating partial shading
Source: Own elaboration

Following the same tests as for the 85W panel we now show the second disturbance in figure (20) of the 100W panel when the battery load is increased and we observe that the control is still operating correctly as the panel voltage Vpv is still smoothly at the reference voltage Vref now at 18.6V.

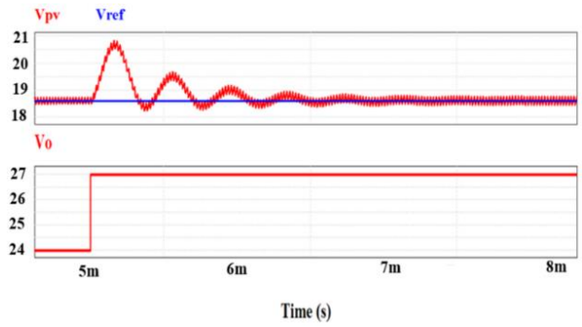

Figure 20 Second disturbance present in the battery
Source: Own elaboration

Conclusion

In conclusion, following the theoretical analysis and verifying with the simulations we can see that it is possible to regulate the input voltage of the two photovoltaic panels with the application of a PI controller, using the MATLAB tool for the design itself, therefore, we can also say that the use of this tool greatly facilitates the design of controllers for application in switched converters, and that it meets the objectives set for this research in an optimal way, It could also be observed that as mentioned in the introduction, implemented a conventional PI control we can have the same performance of a much more robust control, applied in photovoltaic systems, having as advantages the easy application, reduced operating time and reduced operating costs when the model is implemented physically, the following research work will be the application of the MPPT algorithm based on the method Perturb and Observe how in Méndez et al. , (2015) in the same way on both PV panels, and the physical implementation of the system.

References

Alam, K., & Hoque, A. (2019). Design and Analysis of Closed Loop Interleaved Boost Converter with Arduino based Soft PI Controller for Photovoltiac Application. Proceedings of 2019 3rd IEEE International Conference on Electrical, Computer and Communication Technologies, ICECCT 2019, 1–5. DOI: https://doi.org/10.1109/ICECCT.2019.8869408

ISSN 2523-6873
ECORFAN® All rights reserved.

Bouchakour, A., Zaghba, L., Brahami, M., & Borni, A. (2015). Study of a Photovoltaic System Using MPPT Buck-Boost Converter. International Journal of Materials, Mechanics and Manufacturing, 3(1), 65–68. DOI: https://doi.org/10.7763/ijmmm.2015.v3.168

Dhople, S. V., Davoudi, A., & Chapman, P. L. (2009). Steady-state characterization of multi-phase, interleaved Dc-Dc converters for photovoltaic applications. 2009 IEEE Energy Conversion Congress and Exposition, ECCE 2009, 330–336. DOI: https://doi.org/10.1109/ECCE.2009.5316415

Dwivedi, L. K., & Saket, R. K. (2017). Improve efficiency of Photovoltaic (PV) system based by PID controller. International Research Journal of Engineering and Technology, 4(5), 2273–2277.

Ebrahimi, M. J., & Viki, A. H. (2015). Interleaved high step-up DCDC converter with diode-capacitor multiplier cell and ripple-free input current. International Journal of Renewable Energy Research, 5(3), 782–788. DOI: https://doi.org/10.11591/eei.v4i4.512

Hogan, N. (2014). A general actuator model based on nonlinear equivalent networks. IEEE/ASME Transactions on Mechatronics, 19(6), 1929–1939. DOI: https://doi.org/10.1109/TMECH.2013.2294096

Leuchter, J., Zaplatilek, K., & Bauer, P. (2012). Photovoltaic model for circuit simulation. IECON Proceedings (Industrial Electronics Conference), 5399–5405. DOI: https://doi.org/10.1109/IECON.2012.6389526

Méndez Díaz, J. F. (2018). Desarrollo de un Sistema de Iluminación Solar Para el Ahorro de Energía Eléctrica en el Alumbrado Público de México. Universitat Rovira i Virgili, Universidad Popular Autónoma del Estado de Puebla

Mendez-Diaz, F., Pico, B., Vidal-Idiarte, E., Calvente, J., & Giral, R. (2019). HM/PWM Seamless Control of a Bidirectional Buck-Boost Converter for a Photovoltaic Application. IEEE Transactions on Power Electronics, 34(3), 2887–2899. DOI: https://doi.org/10.1109/TPEL.2018.2843393

Méndez-Diaz, F., Ramirez-Murillo, H., Calvente, J., Pico, B., & Giral, R. (2015). Input voltage sliding mode control of the versatile buck-boost converter for photovoltaic applications. Proceedings of the IEEE International Conference on Industrial Technology, 2015-June(June), 1053–1058. DOI: https://doi.org/10.1109/ICIT.2015.7125236

Méndez-Diaz, F.; Ramirez-Murillo, H.; Garces, P.; Romero, A.; Calvente, J.; Giral, R. (2014). Control en Modo de Deslizamiento de la Tensión de Entrada del Convertidor Buck - Boost. June, 1–6

Rabiaa, O., Mouna, B. H., Lassaad, S., Aymen, F., & Aicha, A. (2019). Cascade Control Loop of DC-DC Boost Converter Using PI Controller. International Symposium on Advanced Electrical and Communication Technologies, ISAECT 2018 - Proceedings, May 2019, 1–5. DOI: https://doi.org/10.1109/ISAECT.2018.8618859

Ram, J. P., Babu, T. S., & Rajasekar, N. (2017). A comprehensive review on solar PV maximum power point tracking techniques. Renewable and Sustainable Energy Reviews, 67, 826–847. DOI: https://doi.org/10.1016/j.rser.2016.09.076

Saravanan, S., & Ramesh Babu, N. (2017). Analysis and implementation of high step-up DC-DC converter for PV based grid application. Applied Energy, 190, 64–72. DOI: https://doi.org/10.1016/j.apenergy.2016.12.094

Sharma, C., & Jain, A. (2015). Modeling of buck converter models in MPPT using PID and FLC. Telkomnika (Telecommunication Computing Electronics and Control), 13(4), 1270–1280. DOI: https://doi.org/10.12928/TELKOMNIKA.v13i4.1774

Taghvaee, M. H., Radzi, M. A. M., Moosavain, S. M., Hizam, H., & Hamiruce Marhaban, M. (2013). A current and future study on non-isolated DC-DC converters for photovoltaic applications. Renewable and Sustainable Energy Reviews, 17, 216–227. DOI: https://doi.org/10.1016/j.rser.2012.09.023

ISSN 2523-6873
ECORFAN® All rights reserved.

Tian, X., Zheng, M., & Yang, S. (2016). Maximum power point tracking for photovoltaic power based on the improved interleaved boost converter. Proceedings of the 2016 IEEE 11th Conference on Industrial Electronics and Applications, ICIEA 2016, 1, 2215–2218. DOI: https://doi.org/10.1109/ICIEA.2016.7603957

ISSN 2523-6873
ECORFAN® All rights reserved.